β-blocker suppresses both tumoral sympathetic neurons and perivascular macrophages during oncolytic herpes virotherapy

Konstantina Kyritsi,[1] Rafal Pacholczyk,[2] Eugene Douglass,[3] Miao Yu,[4] Hui Fang,[2] Gang Zhou [ID] ,[2] Balveen Kaur [ID] ,[1] Qin Wang,[5] David H Munn,[6] Bangxing Hong [ID] [1]

For numbered affiliations see end of article.

Correspondence to
Dr Bangxing Hong;
bhong@augusta.edu

ABSTRACT

Background The autonomic nervous system (ANS) plays a key role in regulating tumor development and therapy resistance in various solid tumors. Within the ANS, the sympathetic nervous system (SNS) is typically associated with protumor effects. However, whether the SNS influences the antitumor efficacy of intratumoral injections of oncolytic herpes simplex virus (oHSV) in solid tumors remains unknown.

Methods In this study, we examined SNS innervation and its interaction with immune cell infiltration in both human and murine triple-negative breast cancer models during intratumoral oHSV injections and SNS blockade on oHSV's antitumor activity.

Results Intratumor oHSV injection promotes SNS innervation accompanied by CD45+cell infiltration in both the human MDA-MB-468 orthotopic model and the murine 4T1 mammary tumor model. Mechanistically, tumor-secreted factors vascular endothelial growth factor (VEGF), platelet-derived growth factor (PDGF), and transforming growth factor beta (TGF-β) and transcription factors (CREB, AP-1, MeCP2, and REST), which promote SNS innervation, were found to be upregulated in oHSV-treated tumors. Combining the SNS antagonist, a β-blocker, with oHSV significantly increased immune cell infiltration, particularly CD8+T cells in oHSV-treated 4T1 tumors. Single-cell messenger RNA sequencing revealed that oHSV injection upregulated a specific population of perivascular macrophages (pvMacs) expressing high levels of VEGFA, CD206, CCL3, and CCL4, which suppress T-cell activation. The use of a β-blocker reduced the infiltration of oHSV-induced pvMacs, transition to inflammatory macrophages expressing Hexb, enhancing the diversity of T-cell receptor clonotypes. Further analysis suggested that TGF-β signaling within the tumor partially mediates SNS activation in the 4T1 model.

Conclusion Our findings demonstrate that combining a β-blocker with oHSV significantly enhances the antitumor efficacy of oHSV in breast cancer by targeting TGF-β-mediated SNS innervation and immunosuppression.

INTRODUCTION

The sympathetic nervous system (SNS), a division of the peripheral autonomic nervous

WHAT IS ALREADY KNOWN ON THIS TOPIC

⇒ The sympathetic nervous system (SNS) not only plays a direct role in regulating tumorigenesis but also influences immune cell function, including T cells and antigen-presenting cells, both directly and indirectly. Within the tumor microenvironment, the SNS has been shown to contribute to T-cell exhaustion.

WHAT THIS STUDY ADDS

⇒ The impact of SNS on tumor therapy resistance remains poorly understood. This study investigates the effects of SNS on the breast cancer microenvironment and the antitumor immune response during oncolytic virotherapy. The findings suggest that oncolytic virotherapy can regulate the activity of both tumor-infiltrating T cells and myeloid cells. Furthermore, blocking SNS activity using beta-blockers enhances the antitumor effects of oncolytic virotherapy.

HOW THIS STUDY MIGHT AFFECT RESEARCH, PRACTICE OR POLICY

⇒ This study highlights that intratumoral injection of oncolytic viruses can induce SNS innervation in the tumor and modulate the immunosuppressive tumor microenvironment. Targeting SNS represents a promising strategy to overcome therapy resistance in solid tumors during oncolytic virotherapy.

system (ANS), regulates the physiological "fight-or-flight" response to stress, enhancing tissue defense and physical strength. In both physiological and pathological conditions, the SNS exerts immune regulatory functions through the activation of α-adrenergic and β-adrenergic receptors expressed on CD4+,[1] CD8+,[2] regulatory T (Treg) cells,[3] macrophages,[4] and dendritic cells.[5] Recent studies have shown that the SNS promotes tumor development,[6–8] metastasis,[9] and therapy resistance[2] by releasing catecholamine

neuroeffectors into the tumor microenvironment. These neuroeffectors interact with adrenergic receptors to modulate the functions of tumor cells, stromal cells, and immune cells. Additionally, the SNS has been implicated in controlling the exhaustion of effector and memory T-cell functions.[2]

Oncolytic virotherapy (OV) is a form of immunotherapy developed to target advanced solid tumors that are resistant to standard-of-care (SOC) treatments and other forms of immunotherapy. While OV has been approved for use in metastatic solid tumors, its antitumor efficacy remains limited due to the suppressive tumor microenvironment. Understanding the underlying mechanisms that contribute to OV resistance is critical to improving its effectiveness in solid tumors. Whether SNS innervation influences the antitumor efficacy of OV has yet to be explored.

In this report, we characterize the innervation of the SNS in triple-negative breast cancer (TNBC) models following intratumoral injection of oncolytic herpes simplex virus (oHSV). We systematically investigate the impact of SNS innervation during oHSV therapy on alterations within the tumor microenvironment, with a particular focus on immune cell phenotypes and the signaling pathways governing SNS and immune cell interactions. Furthermore, we explore whether combining the SNS antagonist β-blocker with oHSV enhances its antitumor efficacy.

MATERIALS AND METHODS
Cells, oncolytic virus, and mice
Human breast cancer cells (MDA-MB-468) and mouse breast cancer cells (4T1) were cultured in Dulbecco's Modified Eagle Medium (DMEM) medium supplemented with 10% fetal bovine serum (FBS). The oHSV used in this study is a double mutant (ICP6 and gamma 34.5) of HSV serotype 1. The oHSV expressed green fluorescent protein (GFP), which can be used to monitor its infection in breast cancer. Human breast cancer MDA-MB-468 cells are more sensitive to oHSV infection and oncolysis compared with mouse breast cancer 4T1 cells (online supplemental file 1). This increased sensitivity is attributed to the expression of nectin-1, a receptor for HSV infection, on human cells.[10] Female athymic nude mice (JAX#002019) and Balb/cJ mice (JAX#000651) were purchased from Jackson Laboratory.

In vivo murine breast cancer model
The human MDA-MB-468 breast cancer model was established by injecting 1×10^5 tumor cells into the mammary gland of 6-week-old female nude mice. The mouse 4T1 breast cancer model was created by injecting 5×10^4 tumor cells into 6-week-old female Balb/cJ mice. When tumors reached 6–8 mm in diameter, tumor-bearing mice were intratumorally injected with phosphate-buffered saline (PBS) or 5×10^5 infectious units of oHSV, with or without intraperitoneal treatment with a β-blocker (2 mg/

kg/day propranolol, Cayman Chemical)[11] until analysis. This study was approved by the Institutional Animal Care and Use Committee of Augusta University.

Flow cytometry analysis
For cell surface staining, cells were washed with PBS and blocked with an Fc blocker (BD Biosciences, San Jose, California, USA). Fluorochrome-labeled antibodies (CD45, CD4, CD8, F4/80, CD44, CD206) were obtained from BD Biosciences (Franklin Lakes, New Jersey, USA), added, and stained for 30 min as previously described.[12] All samples were analyzed using a CytoFLEX flow cytometer (Beckman Coulter, California, USA).

Immunofluorescence staining
Human and mouse breast cancer tissues were collected, and paraffin blocks were prepared. After deparaffinization and antigen retrieval, sections were permeabilized with 0.04% Triton-X and blocked with 2% goat serum. Primary antibodies (ICP4, 1:100; TH, 1:100; CD45, 1:200; CD3, 1:100; cleaved caspase-3, 1:150; CD8, 1:100; and Ki-67, 1:200), obtained from Abcam (Cambridge, UK), were diluted in 0.4% bovine serum albumin (BSA) and incubated overnight at 4°C. Following washing, sections were incubated with secondary antibodies for 1 hour. Images were captured using a fluorescence microscope (Nikon Eclipse Ts2).

Quantitative RT-PCR
PBS-treated or oHSV-treated 4T1 tumors, with or without β-blocker treatment, were harvested, and messenger RNA (mRNA) was extracted using the Qiagen RNeasy kit. Complementary DNA (cDNA) was synthesized using the High-Capacity cDNA Reverse Transcription Kit (Applied Biosystems). Quantitative reverse transcription-polymerase chain reaction (RT-PCR) was performed using SYBR Green methods. Gene-specific primers (sequences listed in online supplemental table 1) were synthesized by Integrated DNA Technologies (IDT, Coralville, Iowa, USA).

RNA library construction and data analysis
For bulk mRNA sequencing (mRNA-seq), total RNA was extracted from PBS-treated or oHSV-treated 4T1 tumors with or without β-blocker treatment using the RNeasy Mini Kit (#74104, Qiagen, Germany). RNA sequencing (RNA-seq) library was constructed by the Augusta University Genomics Core according to the manufacturer's instructions for Takara SMARTer Stranded Total RNA Sample prep Kit (634876, Takara Bio USA). RNA-seq data were generated using an Illumina NovaSeq 6000 with a 100 bp paired-end read format.

Raw mRNA sequence reads were pre-processed using Cutadapt (V.1.15) to remove bases with quality scores <20 and adapter sequences. Clean RNA-seq reads were aligned to the reference genome (GRCh38.83) using STAR (V.2.5.3a).[13] Gene abundance was measured using HTSeq-count to obtain the uniquely mapped read number, with annotations from ENSEMBL V.83. Only

genes with >5 reads in at least one sample were included in differential expression analysis using DESeq2,[14] which implements a negative binomial distribution model. Resulting p values were adjusted using the Benjamini and Hochberg method[15] to control for false discovery rates (FDR). Genes with FDR<0.05 were considered differentially expressed for further analysis. Gene Set Enrichment Analysis was performed using the RDAVID WebService (V.1.19.0)[16] for Gene Ontology terms and the R package for Kyoto Encyclopedia of Genes and Genomes (KEGG) pathway analysis. Enrichment p values were adjusted using the Benjamini and Hochberg method.

Single-cell mRNA sequencing and T-cell receptor sequencing

CD45+cells were isolated from 4T1 tumors treated with oHSV and β-blocker. mRNA libraries were constructed using the 10x Genomics Chromium Next GEM Single Cell 5' HT Reagent Kits V.2 (Dual Index). Raw sequencing data files were demultiplexed into FASTQ files and analyzed using the Cell Ranger algorithm (10x Genomics). The filtered count matrices and filtered contig V(D)J annotations were analyzed with R (V.4.2) using Seurat and Bioconductor packages. The low-quality cells were filtered out retaining cells with detected gene numbers >200, and mitochondrial genes <15%. Genes that were expressed by less than 3 cells were rejected.

For T-cell receptor (TCR)-sequencing analysis, the TCR diversity and richness between samples were analyzed using Shannon Index, Normalized Entropy Index and Chao1 index, whereas Shannon Index = $-\sum pi \times \log(pi)$, Normalized Entropy Index = $-\sum pi \times \ln(pi) / \ln(S)$, pi=frequency of i-th clone, S=total number of clones. Normalized entropy is Shannon entropy divided by ln of the total number of clonotypes. The normalized entropy ranges from 0 to 1 with one indicating maximum diversity. Chao1 index is used to measure "Richness", it estimates the total number of species (clones) in the analyzed population. The clonal richness between samples using integrations of rarefaction and extrapolation (prediction) of effective numbers of clonotypes across indicated samples.

Statistical analysis

All quantitative results are presented as means±SD. Statistical differences between two groups were assessed using the Mann-Whitney U test or Student's t-test. For comparisons involving more than two groups, analysis of variance was employed. Statistical analyses were conducted using Prism V.5 software (GraphPad Software, La Jolla, California, USA). A p value of <0.05 was considered statistically significant.

RESULTS

Sympathetic neuron innervation of tumor-infiltrating lymphocytes in tumors from patients with triple-negative breast cancer and a mouse orthotopic breast cancer model

Neuron innervation could not only directly influence tumorigenesis but also modulate tumor-infiltrated immune cell function. Given that SNS innervation regulates immune cell activity in both physiological and pathological conditions,[17] we first analyzed whether SNS signaling could directly or indirectly regulate tumor-infiltrating lymphocytes (TILs) in patients with breast cancer and a mouse orthotopic breast cancer model. Using single-cell RNA sequencing (scRNA-seq) data from human patients with breast cancer, we found that neuronal markers (TUBB3), adrenergic receptors (ADRB2, ADRA2), and SNS innervation factors, such as NGF and NGFR, are ubiquitously detected in patient tumors (online supplemental figure 2). In the human TNBC scRNA-seq data set, the neuronal gene TUBB3 was identified in both tumor cell and endothelial cell clusters (figure 1a,b). Additionally, the adrenergic receptor ADRB2, but not ADRB1, was expressed in both immune cells, including CD4+ and CD8+ T cells, B cells, NK cells, macrophages, and dendritic cells, as well as in non-immune cells, such as endothelial and luminal cells (figure 1a,b). In contrast, the ADRA2A receptor was primarily expressed in non-immune cells, including perivascular-like cells and cancer-associated fibroblasts (CAFs) (figure 1a,b). The differential expression of adrenergic receptors in immune and non-immune cells highlights the variability in the sympathetic nervous system's regulation of breast cancer immunity.

Next, we examined SNS innervation in both human and murine TNBC orthotopic models. Immunofluorescence staining of tyrosine hydroxylase (TH),[2] a marker of SNS, in the mouse 4T1 tumor model in Balb/c mice revealed that SNS primarily innervated the tumor-adjacent mammary gland (MM) and the interface between the mammary gland and tumor tissue (MT) but was absent in the tumor tissue (TU) (figure 1c), which is consistent with a previous study using flow cytometry methods.[18] The MT region was infiltrated by CD45+cells, where the majority of TILs were located (figure 1c). Similarly, TH staining in the human MDA-MB-468 tumor model in nude mice showed SNS innervation in the MM and MT regions, but not in the TU region, although fewer CD45+cells were observed in the MT region (figure 1d). These findings suggest that SNS innervation in the MM and MT regions may directly or indirectly influence TIL function in breast cancer.

To characterize SNS innervation in TILs in the 4T1 breast cancer syngeneic mouse model, single-cell mRNA-seq analysis was performed on CD45-microbead purified TILs (figure 1e). The results revealed that the SNS receptor *Adrb2* is expressed in both T cells and myeloid cells (figure 1e,f). Additionally, SNS innervation factor *Pdgfa* is predominantly expressed in monocytes and macrophages (figure 1g), while *Tgfb1* and *Tgfbr1* are ubiquitously expressed across all TIL populations but show elevated expression in monocytes and macrophages (figure 1g).
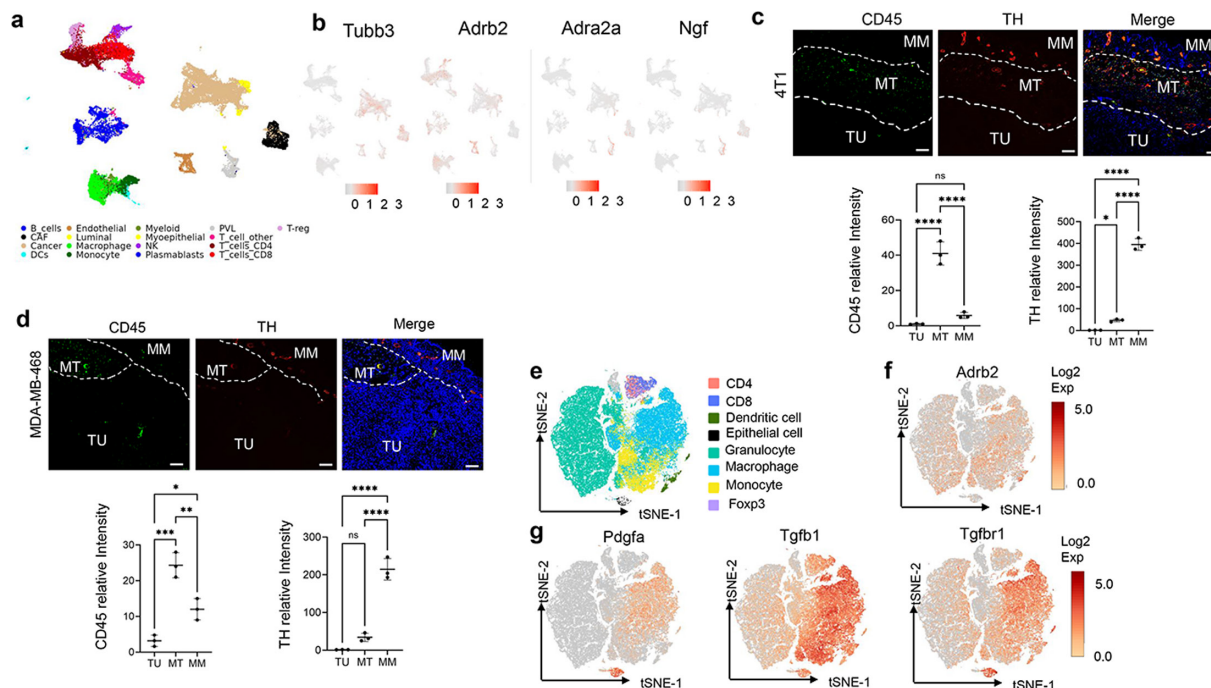
Figure 1 SNS innervation in tumor-infiltrated lymphocytes (TILs), tumor, and tumor stromal cells in breast cancer. (a) t-SNE analysis of different cell clusters in human triple-negative breast cancer single-cell RNA sequencing (scRNA-seq) data. The pan-neuron marker TUBB3, adrenergic receptors (ADRB2 and ADRA2A), and the SNS growth factor NGF were expressed in TILs, including CD4 and CD8 T cells, NK cells, regulatory T cells (Treg), myeloid cells (macrophages and monocytes), tumor cells, and stromal cells (endothelial cells, cancer-associated fibroblasts, and perivascular-like cells (PVL). (c–d) SNS innervation in murine 4T1 and human MDA-MB-468 mammary gland xenograft tumors were detected via immunofluorescence staining for tyrosine hydroxylase (TH) and CD45 to identify immune cells. n=3, *p<0.05, **p<0.01, ***p<0.005, ****p<0.001. (e–g) Mouse breast cancer 4T1 cells were inoculated into the mammary glands of female Balb/c mice. 15 days later, CD45+cells were harvested from the tumors, and scRNA-seq was performed. Subtypes of immune cells (e), adrenergic receptor ADRB2 (f), and adrenergic neuron growth factors PDGF-α, TGF-β1, and TGFBR1 (g) were identified in the TILs through t-SNE analysis. CAFs, cancer-associated fibroblasts; DCs, dendritic cells; MM, mammary gland; MT, mammary gland and tumor tissue; PDGF, platelet-derived growth factor; SNS, sympathetic nervous system; TGF, transforming growth factor; t-SNE, t-distributed Stochastic Neighbor Embedding; TU, tumor tissue.

Increased SNS innervation adjacent to oHSV infection in mouse orthotopic TNBC models

To characterize the effects of oHSV therapy on SNS activation in breast cancer, we intratumorally treated mouse orthotopic 4T1 tumors in Balb/c mice with oHSV. Bulk tumor mRNA-seq analysis demonstrated that oHSV treatment significantly increased signaling pathways associated with oncogenesis and tumor cell growth, specifically the PI3K-AKT-mTOR and mTORC1 pathways (figure 2a). Additionally, oHSV treatment upregulated user-defined gene signatures associated with SNS innervation (figure 2b). Analysis of adrenergic receptors revealed significant upregulation of both ADRB1 and ADRB2 in tumors following intratumoral injection of oHSV (figure 2c). Furthermore, oHSV intratumoral injection enhanced the release of SNS innervation factors, including nerve growth factor (NGF),[19] vascular endothelial growth factor (VEGF),[20] platelet-derived growth factor (PDGF),[21] and transforming growth factor beta (TGF-β)[22] (figure 2d). Transcription factors that positively or negatively regulate SNS activation, such as CREB,[23] AP-1,[24] and MeCP2,[25] were also found to be highly

upregulated in the 4T1 tumors after oHSV injection (online supplemental figure 3).

Next, we investigated SNS innervation in 4T1 tumors following intratumor injection of oHSV using immunofluorescence staining for tyrosine hydroxylase (TH) and the HSV-infected cell polypeptide 4 (ICP4)[12] as indicators of SNS and oHSV infection, respectively. Our results demonstrated a significantly higher level of SNS innervation in tumors infected with oHSV (figure 2e,f). In contrast, TH+cells were not detected in tumors of vehicle-treated mice (figure 2e,f). Further analysis revealed a positive correlation between the intensity of TH neuron innervation and oHSV infection, suggesting that TH+neuron innervation is closely associated with areas of oHSV infection (figure 2g, online supplemental figure 4a).

To determine whether the increase in SNS innervation observed during oHSV treatment in TNBC is dependent on adaptive immunity, we analyzed TH+neuron innervation in human TNBC MDA-MB-468 xenografts in the mammary glands of female nude mice. Intratumoral injection of oHSV significantly increased TH+neuron innervation both within
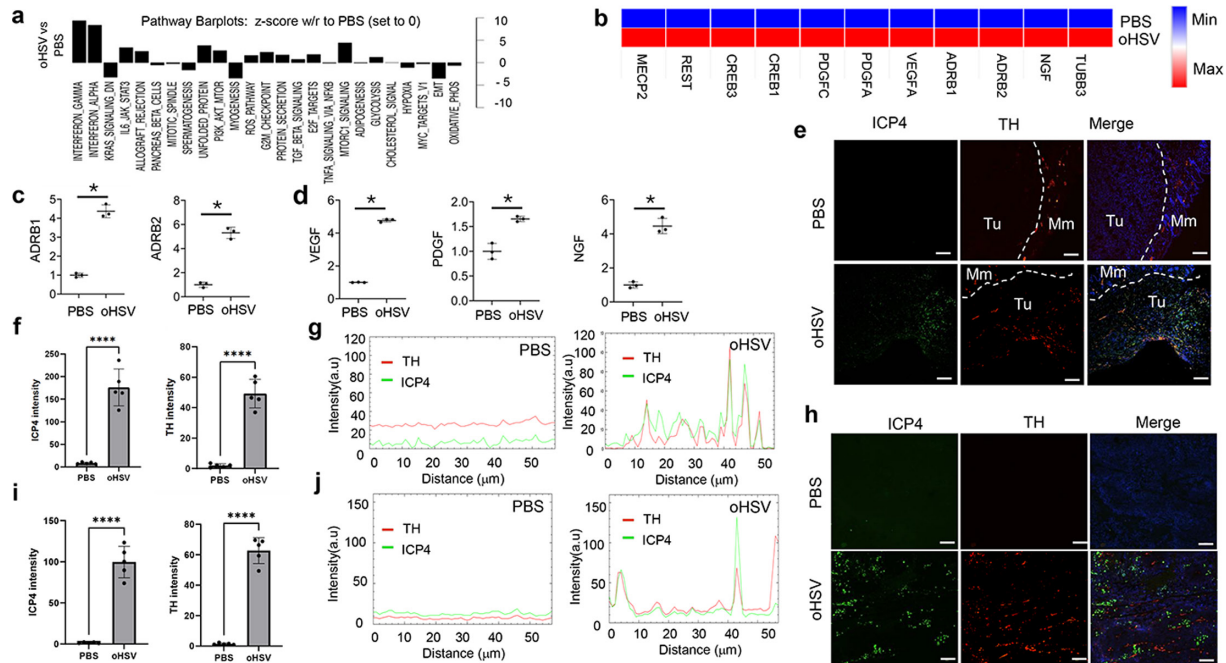
Figure 2 Intratumor oHSV treatment enhances SNS innervation in breast cancer. Bulk tumor mRNA sequencing analysis (a–b) and quantitative reverse transcription-polymerase chain reaction (RT-PCR) analysis of adrenergic receptors ADRB1 and ADRB2 (c) and SNS growth factors vascular endothelial growth factor (VEGF), platelet-derived growth factor (PDGF), and neuron growth factor (NGF) (d) were conducted in murine 4T1 mammary gland tumors in Balb/c mice 3 days following intratumor injection of oHSV (n=3, *p<0.05). oHSV infection and SNS innervation in 4T1 mammary tumors were assessed through immunofluorescence staining of ICP4 and TH, respectively (e–g). The relative fluorescence intensity (f, n=3, *p<0.05) and spatial correlation (g) of ICP4 and TH after oHSV intratumor injection were quantified using ImageJ. Human TNBC MDA-MB-468 mammary tumors in nude mice were treated intratumorally with 5×10^5 oHSV. oHSV infection and SNS innervation in tumor-bearing mice were analyzed through immunofluorescence staining of ICP4 and TH (h). The density of TH and ICP4 immunofluorescence staining was quantified using ImageJ (i, n=3, *p<0.05). The spatial distribution of oHSV infection (ICP4) and SNS innervation (TH) was analyzed using ImageJ (j). ICP4, infected cell polypeptide 4; Mm, mammary gland; oHSV, oncolytic herpes simplex virus; PBS, phosphate-buffered saline; PDGF, platelet-derived growth factor; RT-PCR, reverse transcription-polymerase chain reaction; SNS, sympathetic nervous system; TGF, transforming growth factor; TH, tyrosine hydroxylase; TNBC, triple-negative breast cancer; Tu, tumor. bar, 100μm; VEGF, vascular endothelial growth factor.

the tumor and in the adjacent mammary gland (figure 2h,i). In contrast, vehicle-treated mice exhibited sympathetic neuron innervation only in the adjacent mammary gland, with no innervation in the tumor region (figure 2h,i). Furthermore, the intensity of TH+neuron innervation was positively correlated with the extent of oHSV infection (figure 2j, online supplemental figure 4b).

These results suggest that while the immune response may influence SNS innervation in breast cancer, the enhancement of sympathetic neuron innervation during intratumoral oHSV treatment occurs independently of the immune response.

TH+ neuron innervation accompanied CD45+ cell infiltration following intratumoral injection of oHSV

The injection of oHSV not only induces inflammation in the virus-infected tumor area but also promotes local immune cell infiltration. Immune cell infiltration consistently coincides with oHSV-infected tumor sites. We next investigated whether CD45+immune cell infiltration in oHSV-infected tumors is spatially correlated with TH+neuron innervation. In 4T1 tumor-bearing Balb/c mice, intratumoral injection of oHSV significantly increased CD45+cell infiltration (figure 3a,b). H&E staining and immunohistochemistry staining of TUBB3 indicate that neuron innervation not only exists in adjacent mammary gland but also inside the tumor[18 26] (Online supplemental figure 5). In contrast, TH+neurons are predominantly present in the tumor-adjacent mammary gland in untreated tumors (figure 1c). TH+SNS innervation was present at sites of CD45+cell infiltration (figure 3a and c) inside oHSV-treated tumors, suggesting that the closer the SNS innervation is to CD45+cells, the stronger the intensity of TH+innervation.

Although nude mice implanted with human MDA-MB-468 tumors lack functional T and B cells, myeloid cells still infiltrate the tumors, contributing to tumor progression and resistance to therapy. We examined the infiltration of CD45+cells in human MDA-MB-468 xenografts implanted in the mammary glands of these mice. Intratumoral injections of oHSV not only enhance TH+sympathetic neuron innervation in the virus-infected region (figure 2f), but also promote the infiltration of CD45+cells within the same area (figure 3d,e). Further analysis revealed a
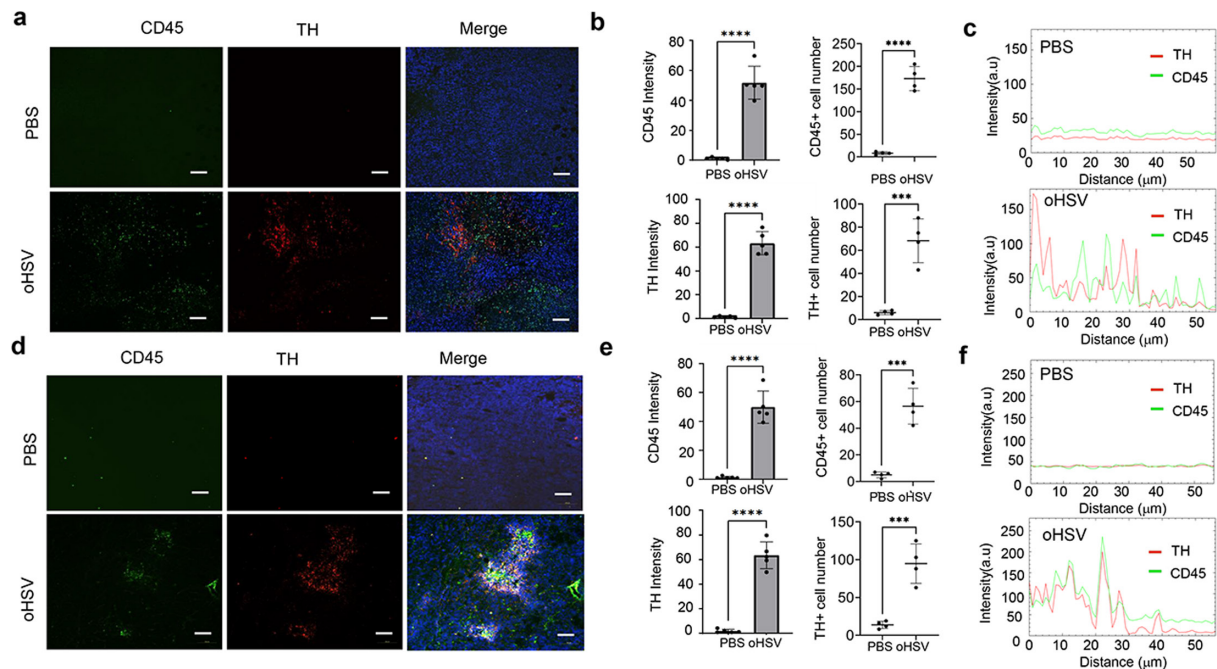
Figure 3 Intratumor injection of oHSV increases CD45+cell infiltration adjacent to SNS innervation of the tumor. Murine 4T1 mammary tumors were intratumorally injected with 5×10^5 oHSV or PBS. CD45+cell infiltration and TH+SNS innervation in the tumor were assessed through immunofluorescence staining (a–c). The relative CD45 and TH fluorescence intensity, CD45+ and TH+cell number (b, n=4, ***p<0.005, ****p<0.001) and spatial correlation (c) of CD45 and TH after oHSV intratumor injection were quantified using ImageJ. Human MDA-MB-468 mammary tumors were also treated with 5×10^5 oHSV or PBS. CD45+cell infiltration and TH+SNS innervation in these tumors were analyzed by immunofluorescence staining (d–f). The CD45 and TH fluorescence intensity, CD45+ and TH+cell number (e, n=4, ***p<0.005, ****p<0.001) and spatial correlation (f) of CD45 and TH after oHSV intratumor injection were quantified using ImageJ. bar, 100µm; oHSV, oncolytic herpes simplex virus; PBS, phosphate-buffered saline; SNS, sympathetic nervous system; TH, tyrosine hydroxylase.

correlation between the intensity of TH+neuron innervation and the proximity of CD45+cells (figure 3d and f).

β-blocker enhances the antitumor efficacy of intratumoral oHSV injection in a breast cancer model

Our preliminary findings demonstrated that intratumoral injection of oHSV induces immune cell infiltration and is accompanied by sympathetic neuron innervation in the virus-infected area. We next investigated whether the combination of a β-blocker (a sympathetic neuron antagonist) could influence the antitumor efficacy of oHSV.

In the 4T1 breast cancer model, the combination of intratumoral oHSV injection with systemic delivery of a β-blocker significantly inhibited tumor growth (figure 4a,b). Analysis of TILs revealed that this combination markedly increased immune cell infiltration, particularly CD3+T cells (figure 4c,d). Tumor cell death, induced by both oHSV-mediated oncolysis and immune cell-mediated cytotoxicity, was assessed using cleaved caspase-3 staining. The combination of β-blocker with oHSV significantly enhanced tumor cell death in the 4T1 immunocompetent mouse model (figure 4c–e).

We further investigated the neuronal growth factors that regulate TH+neuron innervation in 4T1 tumors treated with oHSV and β-blockers. Quantification of both secreted factors and transcription factors involved in SNS innervation revealed a feedback upregulation of several key factors, including VEGF, PDGF, CREB, AP-1, REST, and MeCP2, in 4T1 tumors treated with the combination of oHSV and β-blocker (figure 4f,g).

β-blocker modulates immune status in 4T1 tumors following intratumoral oHSV injection

Next, we aimed to investigate how β-blocker administration influences the immune status of 4T1 tumors after intratumoral injection of oHSV. Tumor cell growth and CD8+T cell proliferation in the tumor microenvironment were analyzed using Ki-67 immunofluorescence staining. The results demonstrated that the combination of oHSV with β-blocker significantly reduced tumor cell growth (Ki67+CD8−) compared with treatment with either agent alone (figure 5a,b). Additionally, analysis of CD8+T cell infiltration revealed that the combination treatment significantly enhanced CD8+T cell infiltration within the tumor (figure 5a–c). Furthermore, the combination of oHSV and β-blocker markedly increased CD44 expression in tumor-infiltrating CD4+ and CD8+ T cells (figure 5d,e), indicating activation of these T cells. TCR sequencing demonstrated that the combination of β-blocker and oHSV led to an increase in overall TCR diversity (abundance of TCR clones) (figure 5f and online supplemental figure 6), contributing to immune-mediated tumor cell lysis.[27][28] These findings suggest that the β-blocker not only modulates the sympathetic nervous system within the tumor but also exerts antitumor effects by activating an antitumor immune response.
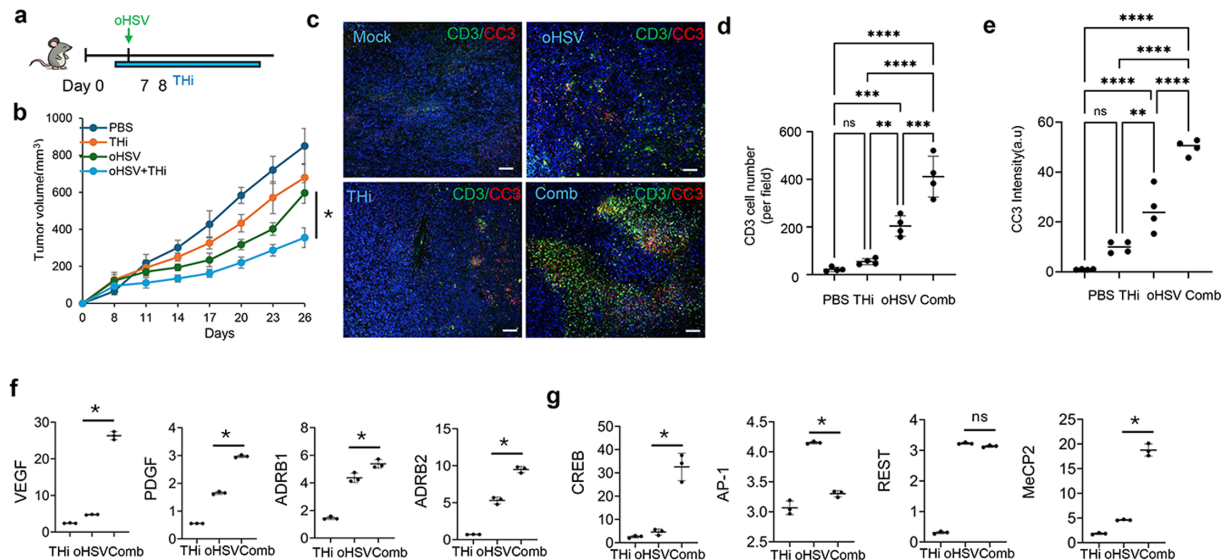
Figure 4 Combination of adrenergic β-blocker with oHSV increases antitumor efficacy. (a) Experimental design. (b) Growth of 4T1 tumors following treatment with the combination of oHSV and adrenergic β-blocker. n=5, *p<0.05. (c) Immunofluorescence staining for T-cell infiltration and tumor cell death, using CD3 and cleaved caspase-3 (CC3) antibodies, respectively. The CD3+cell number (d) and CC3 immunofluorescence intensity (e) were quantified using ImageJ. n=4, **p<0.01, ***p<0.005, ****p<0.0001, ns=no significance. (f–g) Quantitative reverse transcription-polymerase chain reaction (RT-PCR) analysis of adrenergic receptors and SNS growth factors vascular endothelial growth factor (VEGF), platelet-derived growth factor (PDGF) (f), adrenergic receptors ADRB1 and ADRB2 (f), and transcription factors REST, MeCP2, CREB, and AP-1 (g) that regulate SNS innervation. n=3, *p<0.05. Comb, oHSV+THi;oHSV, oncolytic herpes simplex virus; PBS, phosphate-buffered saline; PDGF, platelet-derived growth factor; RT-PCR, reverse transcription-polymerase chain reaxtion; SNS, sympathetic nervous system; THi, β-blocker; VEGF, vascular endothelial growth factor.

Analysis of myeloid cells, specifically tumor-associated macrophages (TAMs), showed that the addition of a β-blocker during oHSV treatment significantly downregulated CD206 expression in TAMs, suggesting a shift from an immunosuppressive to an inflammatory TAM phenotype (figure 5g,h).

β-blocker modulates perivascular macrophage phenotype in oHSV-treated 4T1 tumor microenvironment

To further investigate the mechanisms by which CD8+T cells are regulated in 4T1 tumors during the combination treatment with oHSV and β-blocker, we re-clustered the major myeloid cell populations in the 4T1 tumor using the prediction-from-MetaReference algorithm. This analysis identified the perivascular macrophages (pvMac) population,[29] a subset of macrophage known to regulate tumor growth, invasion, and metastasis through interactions with other cells in the tumor microenvironment (figure 6a,b). Since β-blockers are intended to restore normal vascular architecture and have potential anti-angiogenic effects,[30] we examined the impact of the combination therapy on the pvMac population within TILs. Our results revealed a specific pvMac subpopulation in tumors treated with oHSV, which was depleted when combined with β-blocker treatment (figure 6a,b). This oHSV-induced pvMac subpopulation expressed high levels of Vegfa, Mrc1, Ccl3, and Ccl4 (figure 6c), which are involved in suppressing the activation of other immune cells, including antigen-specific T cells.[31] We further analyzed the monocytes and macrophages (MoMac; clusters 2, 5, 8, 9, and 11 from the scRNA-seq data) within TILs from 4T1 tumors (figure 6d, online supplemental figure 7). Our findings revealed that the combination therapy induced a pro-inflammatory macrophage subtype (figure 6d) characterized by the expression of classical inflammatory markers, including S100a8, S100a9, IL1β, and G0s2 (figure 6e), as well as the novel molecule Hexb (figure 6e,f). To assess the phenotypic transition of tumor-infiltrating macrophages from pvMacs to proinflammatory macrophages, we performed pseudotime analysis on the MoMac clusters (figure 6g). The results indicated that the combination therapy shifted macrophage trajectory from pvMacs to pro-inflammatory macrophages (figure 6g), with a concurrent increase in Hexb expression during this phenotypic transition (figure 6h).

TGF-β signaling partially contributes to the enhanced immune phenotype during combination treatment with β-blocker and oHSV

TGF-β plays a dual role in the tumor microenvironment, promoting both neurogenesis and immunosuppression.[25] scRNA-seq analysis revealed that TGF-β1-3 and TGFBR1-3 are highly expressed in human patients with breast cancer (figure 7a). Further analysis in TNBC using scRNA-seq showed that TGFBR2 and TGFBR3 are prominently expressed in various immune cell clusters, including CD4+T cells, CD8+T cells, and Tregs (figure 7b). This expression pattern closely mirrors that of ADBR2 (figure 1b), suggesting a potential interaction between TGF-β signaling and SNS-ADBR signaling in
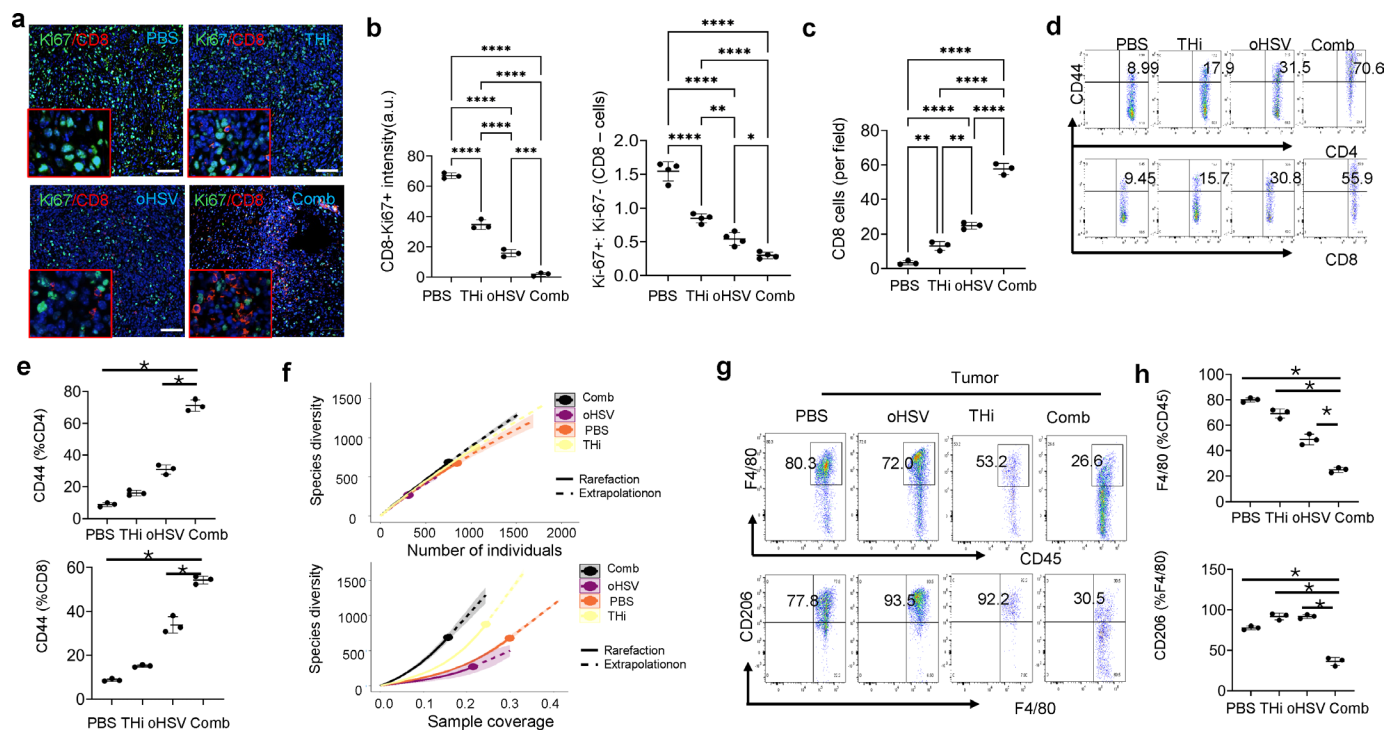
Figure 5 β-blocker enhances CD8 T-cell-mediated anti-tumor immune response during intratumor treatment with oHSV. Balb/c mammary gland 4T1 tumors were treated with the combination of oHSV and β-blocker. 9 days post-treatment, tumor cell proliferation and CD8 T-cell infiltration were analyzed via immunofluorescence staining for CD8 and Ki-67, respectively (a–c). The immunofluorescence intensity of Ki-67 on CD8⁻ cells (CD8-Ki67+, b, n=4), the ratio of Ki-67+ and Ki-67− in CD8⁻ cells (Ki67+: Ki67−, b, n=4), and CD8 T-cell infiltration (c, n=3) were quantified. *p<0.05, **p<0.01, ***p<0.005, ****p<0.0001. (d–e) TILs were also harvested for flow cytometry analysis, evaluating CD4 and CD8 T-cell activation via CD44 staining. n=3, *p<0.05. Estimation of T-cell receptor clonal richness, using the abundance of clones across samples. The sample-size-based and coverage-based integrations of rarefaction and extrapolation (prediction) of effective numbers of clonotypes across indicated samples. Values were calculated using the scRepertoire V.2.0.5 R package (R V.4.4.1). (f) Tumor-infiltrated macrophages were assessed for F4/80+CD206+ expression by flow cytometry (g–h). (h, n=3, *p<0.05). Comb, oHSV+THi; oHSV, oncolytic herpes simplex virus; PBS, phosphate-buffered saline; THi, β-blocker.

immune cells, including CD4+ and CD8+ T cells, as well as Tregs.

We next explored whether TGF-β signaling contributes to the enhanced antitumor efficacy observed with the combination of oHSV and β-blocker in the 4T1 tumor model. Quantitative RT-PCR of secreted factors and transcription factors related to adrenergic neuron growth demonstrated that β-blocker treatment increased the expression of these factors, including TGF-β1(figure 4f,g). The combination of oHSV with β-blocker further amplified these factors while reducing TGF-β1 expression (figure 4f,g, figure 7c). ELISA assays confirmed a significant decrease in TGF-β1 levels during combination therapy compared with single-agent treatment (figure 7d).

Bulk tumor mRNA-seq analysis revealed that β-blocker treatment (TH inhibition) suppressed TGF-β signaling and pathways associated with tumor growth, such as PI3K-AKT-mTOR and mTORC1 signaling. The combination therapy further inhibited oHSV-induced upregulation of these pathways, which are related to tumorigenesis, tumor growth, and therapy resistance (figure 7e).

To further confirm that the reduction in TGF-β signaling contributes to the efficacy of the combination

therapy, we employed a TGF-β blocking antibody. While the combination of oHSV with the TGF-β blocking antibody inhibited tumor growth, it was not as effective as the combination of oHSV with β-blocker (figure 7f).

DISCUSSION

In this study, we found that intratumoral injection of oHSV in both the human TNBC MDA-MB-468 xenograft model in nude mice and the murine 4T1 breast cancer orthotopic model in Balb/c mice increased the production of neurotropic factors and promoted TH+neuron innervation and pvMac infiltration during oHSV therapy. TH+neuron growth was accompanied by myeloid cell infiltration in the MDA-MB-468 nude mice model, and both granulocytes and CD3+T cells in the oHSV-injected 4T1 murine model. TGF-β emerged as a key factor contributing to SNS activation and immunosuppression during oHSV treatment. The combination of a β-blocker with oHSV not only enhanced antitumor efficacy in the 4T1 model by reducing pvMac infiltration and increasing macrophage phenotype transition and CD8+T cells infiltration within the tumor but also increased TCR diversity (figure 7g).
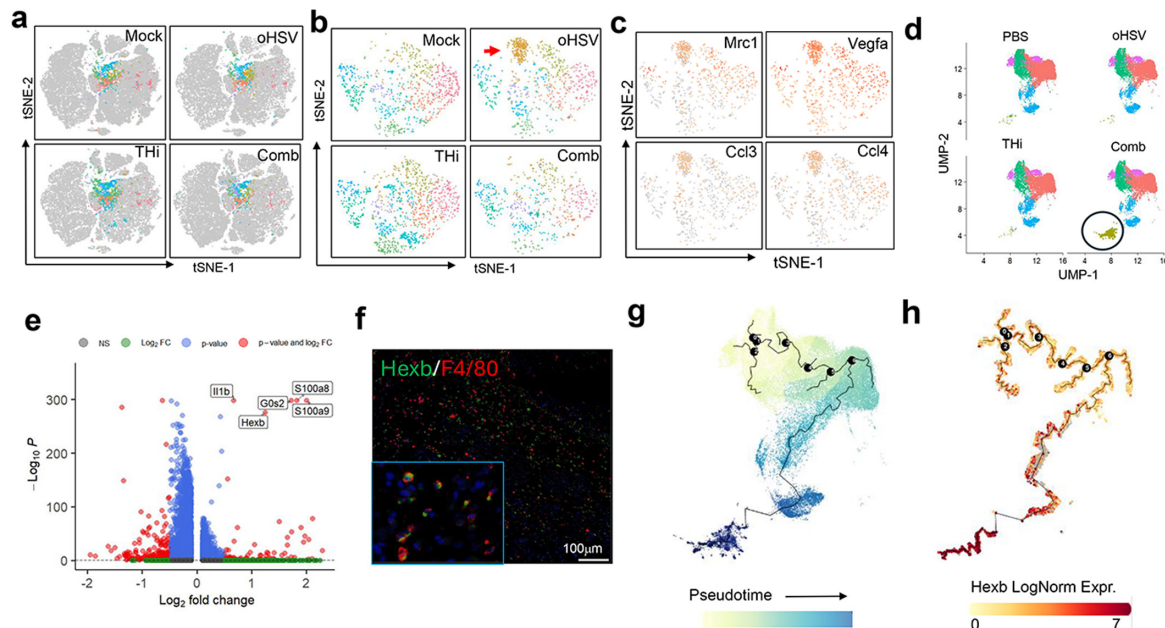
Figure 6 β-blocker modifies both myeloid and T-cell phenotypes in oHSV-treated 4T1 tumors. Balb/c mammary gland 4T1 tumors were treated with the combination of oHSV and β-blocker. Seven days post-treatment, CD45+TILs were harvested from tumors and subjected to scRNA-seq analysis. (a) Clustering of myeloid cells in TILs, referencing published data to identify the pvMac cluster. (b) Re-clustering of pvMac in TILs to identify a specific oHSV-induced pvMac population. (c) Gene signatures of pvMac (Vegfa, Mrc1, Ccl3, and Ccl4) in TILs isolated from oHSV-treated 4T1 tumors. (d) Uniform Manifold Approximation and Projection (UMAP) clustering for monocytes and macrophages (MoMac) from four groups of pooled samples using bBrowser (Bioturing) software. (e) Volcano plot showing differentially expressed genes between Comb sample and all other samples for cells in MoMac clusters shown in (d). Cells in red indicate genes with log2 fold change (log2FC)>0.5 and adjusted p value<0.05. Selected genes are labeled for emphasis. (f) Immunofluorescence staining of Hexb and F4/80 in 4T1 tumor with Comb treatment. (g–h) Pseudotime analysis of MoMac clusters shown in (d), using bBrowser (Monocle3 package). (g) Cells ordered in pseudotime show transition from cluster 9 (monocyte-like cells) through proinflammatory macrophages (clusters 11). (h) Expression of the Hexb gene along the trajectory. The scRNA-seq samples were pooled from five mice for each group. Comb, oHSV+THi; oHSV, oncolytic herpes simplex virus; pvMac, perivascular macrophages; scRNA-seq, single-cell RNA sequencing; t-distributed Stochastic Neighbor Embedding; TILs, tumor-infiltrating lymphocytes; THi, β-blocker; UMAP, Uniform Manifold Approximation and Projection.

Though many factors contribute to the upregulation of neuronal genes in tumor cells,[32 33] tumor stromal and tumor-infiltrated immune cells, many solid tumors, including breast,[18] ovarian,[34] and lung cancers,[35] exhibit multiple types of neuronal innervation within their anatomical location. Sympathetic,[6] parasympathetic,[36] and sensory[7] neurons play distinct roles in tumor development and metastasis. While the SNS is often associated with protumor functions, parasympathetic neurons are typically considered to have antitumor effects. Numerous factors within the tumor microenvironment promote neurogenesis, leading to new neuronal innervation in tumors.[37] The SNS promotes tumor development through multiple mechanisms, including the inhibition of DNA damage repair,[38] mesenchymal activation,[39] oncogene activation,[40] angiogenesis,[11] and the stimulation of proinflammatory responses.[41] These effects may result from neurotransmitters binding directly to receptors on other tumor-associated cell types or indirectly via neuronal innervation.

Perineural invasion (PNI), a process in which cancer cells infiltrate around nerves to reach adjacent or distant organs, has been reported in many cancers, including head and neck[42] and pancreatic cancers,[43] where these organs are innervated by both sympathetic and parasympathetic nerves. PNI can occur prior to lymphatic or vascular invasion,[44] even when the anatomical proximity of nerves to the lymphatic and vascular systems is considered. Our results suggest that oncolytic virotherapies can modulate the tumor microenvironment in ways that favor SNS signaling in CD45+tumor-infiltrating cells, potentially modulating antitumor immune responses. However, the precise mechanisms underlying immune regulation need further exploration.

The SNS regulates immune responses through both direct and indirect pathways. SNS activation can reduce blood flow to lymph nodes and impede leukocyte trafficking within tissues.[45] Direct activation of adrenergic receptors on immune cells has been reported in various cell types, including T cells, where it inhibits their proliferation by suppressing interleukin (IL)-2 production and CD25 expression via cyclic adenosine monophosphate (cAMP)-dependent mechanisms.[46] SNS activation has also been shown to enhance Treg immunosuppressive activity through autocrine/paracrine inhibitory loops,[3] and it can directly inhibit CD8+T cell cytotoxicity.[47] In this study, the
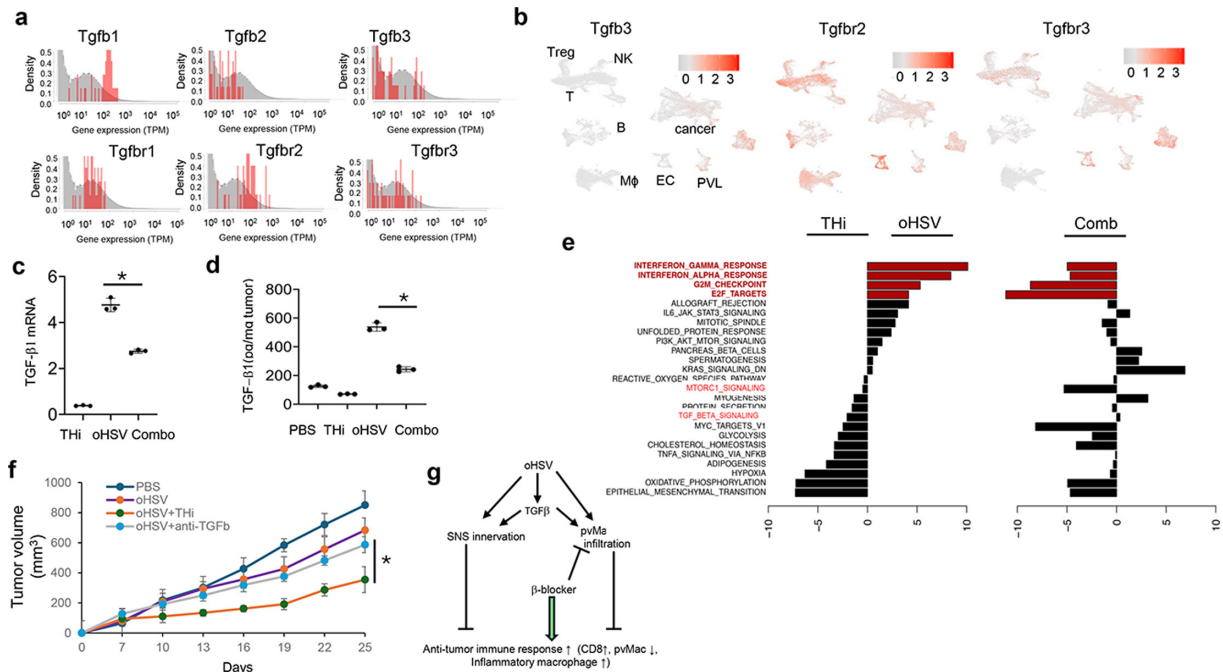
Figure 7 TGF-β is partially responsible for the antitumor efficacy of the combination of oHSV and β-blocker. (a) Single-cell RNA sequencing analysis of TGF-β signaling (TGFB1-3, TGFBR1-3) in human patients with breast cancer. (b) t-SNE plot of TGF-β signaling (TGFB3, TGFBR2-3) in human triple-negative breast cancer tumors. RT-PCR (c, n=3, *p<0.05) and ELISA assay (d, n=3, *p<0.05) for TGF-β1 in murine mammary gland 4T1 tumors treated with oHSV and β-blocker. (e) Bulk tumor mRNA sequencing analysis of 4T1 mammary gland tumors in Balb/c mice 3 days after intratumor injection of oHSV with or without β-blocker. (f) Murine mammary gland 4T1 tumors treated with the combination of oHSV and β-blocker or the combination of oHSV and TGF-β1 antibody. Tumor growth was monitored (n=5, *p<0.05). (g) Graphic abstract of this study. mRNA, messenger RNA; oHSV, oncolytic herpes simplex virus; PBS, phosphate-buffered saline; RT-PCR, reverse transcription-polymerase chain reaction; TGF, transforming growth factor; t-SNE, t-distributed Stochastic Neighbor Embedding; Treg, regulatory T cell.

enhanced function of CD8+T cells following β-adrenergic blockade may be an indirect effect, primarily mediated through the inhibition of TGF-β-driven immunosuppression. Intratumoral injection of oHSV induces inflammation, promotes macrophage-mediated viral clearance, and increases TGF-β production.

TGF-β is a cytokine involved in various biological functions, including immune response, embryonic development, epithelial-mesenchymal transition, and nervous system regulation. In the tumor microenvironment, TGF-β acts as an immunosuppressive cytokine that regulates several immunosuppressive cell populations, including myeloid-derived suppressor cells (MDSCs) and Tregs. TGF-β plays a critical role in maintaining immune tolerance and modulating nervous system function. In the SNS, TGF-β influences the survival, differentiation, and activation of neurons and glial cells, as well as promoting neurite outgrowth in dopaminergic cells.[48] Our study suggests that oHSV infection and replication within tumors promote the secretion of TGF-β by multiple cell types, potentially enhancing neuronal outgrowth. The detailed regulatory mechanisms remain to be studied, but TGF-β has been reported to regulate SNS development by increasing intrinsic neuronal growth capacity.[49] Various cell types within the tumor microenvironment, including tumor cells, endothelial cells, macrophages, and CAFs, are known to produce TGF-β. SOC therapies and immunotherapies can also promote TGF-β production through feedback loops.[50] Further research is needed to elucidate the specific cell types targeted by β-blockers that mediate the inhibition of TGF-β signaling.

TGF-β also contributes to the differentiation of TAMs into pvMacs in the tumor microenvironment.[31 51] CCR2+monocytes/macrophages within tumors adopt a migratory phenotype and localize to the perivascular niche, gaining gene signatures including CD206, VEGFA, Tie2, and Lyve-1, which promote tumor angiogenesis and metastasis.[29] In this study, intratumoral injection of oHSV not only increased immune cell infiltration but also induced the formation of a specific pvMac subpopulation. The addition of a β-blocker significantly reduced pvMac levels in oHSV-treated tumors, suggesting that β-blockers not only inhibit SNS activity within tumors but also influence blood vessel function in tumor angiogenesis. This phenomenon warrants further investigation.

The oHSV used in this study was derived from a virulent HSV strain with genomic deletions of virulence genes, including ICP6 and gamma 34.5, which mediate latent HSV infection in neurons. Our previous studies demonstrated that oHSV can infect induced

pluripotent stem cells (iPSC)-derived neurons without replicating or lysing them.[52] However, local inflammation in oHSV-infected tumors and neurons directly affects tumor-neuron interactions. oHSV infection in tumors not only increases immune cell infiltration but also elevates cytokine secretion (eg, IL-6, TGF-β, and leukemia inhibitory factor (LIF)) in the local tumor environment. These cytokines induce feedback immunosuppression through mechanisms involving MDSCs and Tregs, while also promoting SNS growth in virus-infected tumor regions. In this study, β-blocker treatment inhibited cytokine secretion.

In summary, our study provides new insights into the mechanisms underlying SNS innervation in solid tumors during oHSV therapy, potentially informing the development of novel strategies to enhance the antitumor efficacy of oHSV in solid tumor treatment.

Author affiliations
[1]Department of Pathology, Georgia Cancer Center at Augusta University, Augusta, Georgia, USA
[2]Department of Biochemistry and Molecular Biology, Georgia Cancer Center at Augusta University, Augusta, Georgia, USA
[3]Department of Pharmaceutical and Biomedical Sciences, University of Georgia, Athens, Georgia, USA
[4]Genomics core, Georgia Cancer Center at Augusta University, Augusta, Georgia, USA
[5]Department of Neuroscience & Regenerative Medicine, Augusta University, Augusta, Georgia, USA
[6]Department of Pediatrics, Pediatric Immunotherapy Program, Georgia Cancer Center at Augusta University, Augusta, Georgia, USA

Contributors BH designed experiments. KK, RP, MY, HF, GZ, BK, QW and BH performed the experiment. ED and RP performed bulk mRNA-seq and scRNA-seq analysis. BH wrote the manuscript and DM revised the manuscript. All authors edited and reviewed the manuscript. BH is the guarantor.

Competing interests No, there are no competing interests.

Patient consent for publication Not applicable.

Ethics approval All mice experiments were approved by the institutional Animal Care and Use Committee (IACUC) of Augusta University (no.2023-1098), and by the Institutional Biosafety Committee of Augusta University (no.2308).

Provenance and peer review Not commissioned; externally peer reviewed.

Data availability statement Data are available upon reasonable request.

Supplemental material This content has been supplied by the author(s). It has not been vetted by BMJ Publishing Group Limited (BMJ) and may not have been peer-reviewed. Any opinions or recommendations discussed are solely those of the author(s) and are not endorsed by BMJ. BMJ disclaims all liability and responsibility arising from any reliance placed on the content. Where the content includes any translated material, BMJ does not warrant the accuracy and reliability of the translations (including but not limited to local regulations, clinical guidelines, terminology, drug names and drug dosages), and is not responsible for any error and/or omissions arising from translation and adaptation or otherwise.

ORCID iDs
Gang Zhou http://orcid.org/0000-0001-8967-114X
Balveen Kaur http://orcid.org/0000-0001-7738-0804
Bangxing Hong http://orcid.org/0000-0001-7458-0480

REFERENCES

1 Pilipović I, Vujnović I, Stojić-Vukanić Z, et al. Noradrenaline modulates CD4+ T cell priming in rat experimental autoimmune encephalomyelitis: a role for the α₁-adrenoceptor. *Immunol Res* 2019;67:223–40.
2 Globig A-M, Zhao S, Roginsky J, et al. The β1-adrenergic receptor links sympathetic nerves to T cell exhaustion. *Nature New Biol* 2023;622:383–92.
3 Cosentino M, Fietta AM, Ferrari M, et al. Human CD4+CD25+ regulatory T cells selectively express tyrosine hydroxylase and contain endogenous catecholamines subserving an autocrine/paracrine inhibitory functional loop. *Blood* 2007;109:632–42.
4 Tanner MA, Maitz CA, Grisanti LA. Immune cell beta(2)-adrenergic receptors contribute to the development of heart failure. *Am J Physiol Heart Circ Physiol* 2021;321:H633–49.
5 Takenaka MC, Araujo LP, Maricato JT, et al. Norepinephrine Controls Effector T Cell Differentiation through β2-Adrenergic Receptor-Mediated Inhibition of NF-κB and AP-1 in Dendritic Cells. *J Immunol* 2016;196:637–44.
6 Magnon C, Hall SJ, Lin J, et al. Autonomic nerve development contributes to prostate cancer progression. *Science* 2013;341:1236361.
7 Padmanaban V, Keller I, Seltzer ES, et al. Neuronal substance P drives metastasis through an extracellular RNA-TLR7 axis. *Nature New Biol* 2024;633:207–15.
8 Sloan EK, Priceman SJ, Cox BF, et al. The sympathetic nervous system induces a metastatic switch in primary breast cancer. *Cancer Res* 2010;70:7042–52.
9 Liu D, Yang Z, Wang T, et al. β2-AR signaling controls trastuzumab resistance-dependent pathway. *Oncogene* 2016;35:47–58.
10 Nakashima H, Nguyen T, Kasai K, et al. Toxicity and Efficacy of a Novel GADD34-expressing Oncolytic HSV-1 for the Treatment of Experimental Glioblastoma. *Clin Cancer Res* 2018;24:2574–84.
11 Thaker PH, Han LY, Kamat AA, et al. Chronic stress promotes tumor growth and angiogenesis in a mouse model of ovarian carcinoma. *Nat Med* 2006;12:939–44.
12 Hong B, Sahu U, Mullarkey MP, et al. PKR induces TGF-β and limits oncolytic immune therapy. *J Immunother Cancer* 2023;11:e006164.
13 Dobin A, Davis CA, Schlesinger F, et al. STAR: ultrafast universal RNA-seq aligner. *Bioinformatics* 2013;29:15–21.
14 Anders S, Huber W. Differential expression analysis for sequence count data. *Genome Biol* 2010;11:R106.
15 Benjamini Y, Hochberg Y. Controlling the False Discovery Rate: A Practical and Powerful Approach to Multiple Testing. *Journal of the Royal Statistical Society Series B* 1995;57:289–300.
16 Fresno C, Fernández EA. RDAVIDWebService: a versatile R interface to DAVID. *Bioinformatics* 2013;29:2810–1.
17 Hanoun M, Maryanovich M, Arnal-Estapé A, et al. Neural regulation of hematopoiesis, inflammation, and cancer. *Neuron* 2015;86:360–73.
18 Kaduri M, Sela M, Kagan S, et al. Targeting neurons in the tumor microenvironment with bupivacaine nanoparticles reduces breast cancer progression and metastases. *Sci Adv* 2021;7:eabj5435.
19 Glebova NO, Ginty DD. Heterogeneous requirement of NGF for sympathetic target innervation in vivo. *J Neurosci* 2004;24:743–51.
20 Carmeliet P, Tessier-Lavigne M. Common mechanisms of nerve and blood vessel wiring. *Nature New Biol* 2005;436:193–200.
21 Bi Q, Wang C, Cheng G, et al. Microglia-derived PDGFB promotes neuronal potassium currents to suppress basal sympathetic tonicity and limit hypertension. *Immunity* 2022;55:1466–82.
22 Meyers EA, Kessler JA. TGF-β Family Signaling in Neural and Neuronal Differentiation, Development, and Function. *Cold Spring Harb Perspect Biol* 2017;9:a022244.
23 Parlato R, Otto C, Begus Y, et al. Specific ablation of the transcription factor CREB in sympathetic neurons surprisingly protects against developmentally regulated apoptosis. *Development* 2007;134:1663–70.
24 Nakashima A, Ota A, Sabban EL. Interactions between Egr1 and AP1 factors in regulation of tyrosine hydroxylase transcription. *Brain Res Mol Brain Res* 2003;112:61–9.
25 Mayer SC, Gilsbach R, Preissl S, et al. Adrenergic Repression of the Epigenetic Reader MeCP2 Facilitates Cardiac Adaptation in Chronic Heart Failure. *Circ Res* 2015;117:622–33.
26 Ali SR, Jordan M, Nagarajan P, et al. Nerve Density and Neuronal Biomarkers in Cancer. *Cancers (Basel)* 2022;14:4817.
27 Chung JY-F, Tang PC-T, Chan MK-K, et al. Smad3 is essential for polarization of tumor-associated neutrophils in non-small cell lung carcinoma. *Nat Commun* 2023;14:1794.

28 Kargl J, Busch SE, Yang GHY, *et al*. Neutrophils dominate the immune cell composition in non-small cell lung cancer. *Nat Commun* 2017;8:14381.

29 Opzoomer JW, Anstee JE, Dean I, *et al*. Macrophages orchestrate the expansion of a proangiogenic perivascular niche during cancer progression. *Sci Adv* 2021;7:eabg9518.

30 Cavalu S, *et al*. The multifaceted role of beta-blockers in overcoming cancer progression and drug resistance: Extending beyond cardiovascular disorders. *FASEB J* 2024;38:e23813.

31 Nalio Ramos R, Missolo-Koussou Y, Gerber-Ferder Y, *et al*. Tissue-resident FOLR2+ macrophages associate with CD8+ T cell infiltration in human breast cancer. *Cell* 2022;185:1189–207.

32 Kanojia D, Morshed RA, Zhang L, *et al*. βIII-Tubulin Regulates Breast Cancer Metastases to the Brain. *Mol Cancer Ther* 2015;14:1152–61.

33 Kanojia D, Panek WK, Cordero A, *et al*. BET inhibition increases βIII-tubulin expression and sensitizes metastatic breast cancer in the brain to vinorelbine. *Sci Transl Med* 2020;12:eaax2879.

34 Zhu Y, Zhang G, Yang Y, *et al*. Perineural invasion in early-stage cervical cancer and its relevance following surgery. *Oncol Lett* 2018;15:6555–61.

35 Restaino AC, Walz A, Vermeer SJ, *et al*. Functional neuronal circuits promote disease progression in cancer. *Sci Adv* 2023;9:eade4443.

36 Kamiya A, Hayama Y, Kato S, *et al*. Genetic manipulation of autonomic nerve fiber innervation and activity and its effect on breast cancer progression. *Nat Neurosci* 2019;22:1289–305.

37 Cole SW, Nagaraja AS, Lutgendorf SK, *et al*. Sympathetic nervous system regulation of the tumour microenvironment. *Nat Rev Cancer* 2015;15:563–72.

38 Hara MR, Kovacs JJ, Whalen EJ, *et al*. A stress response pathway regulates DNA damage through β2-adrenoreceptors and β-arrestin-1. *Nature New Biol* 2011;477:349–53.

39 Bruzzone A, Piñero CP, Rojas P, *et al*. α(2)-Adrenoceptors enhance cell proliferation and mammary tumor growth acting through both the stroma and the tumor cells. *Curr Cancer Drug Targets* 2011;11:763–74.

40 Shi M, Liu D, Duan H, *et al*. The β2-adrenergic receptor and Her2 comprise a positive feedback loop in human breast cancer cells. *Breast Cancer Res Treat* 2011;125:351–62.

41 Nilsson MB, Armaiz-Pena G, Takahashi R, *et al*. Stress hormones regulate interleukin-6 expression by human ovarian carcinoma cells through a Src-dependent mechanism. *J Biol Chem* 2007;282:29919–26.

42 Schmitd LB, Perez-Pacheco C, Bellile EL, *et al*. Spatial and Transcriptomic Analysis of Perineural Invasion in Oral Cancer. *Clin Cancer Res* 2022;28:3557–72.

43 Yang M-W, Tao L-Y, Jiang Y-S, *et al*. Perineural Invasion Reprograms the Immune Microenvironment through Cholinergic Signaling in Pancreatic Ductal Adenocarcinoma. *Cancer Res* 2020;80:1991–2003.

44 Saloman JL, Albers KM, Li D, *et al*. Ablation of sensory neurons in a genetic model of pancreatic ductal adenocarcinoma slows initiation and progression of cancer. *Proc Natl Acad Sci U S A* 2016;113:3078–83.

45 Devi S, Alexandre YO, Loi JK, *et al*. Adrenergic regulation of the vasculature impairs leukocyte interstitial migration and suppresses immune responses. *Immunity* 2021;54:1219–30.

46 Sanders VM, Baker RA, Ramer-Quinn DS, *et al*. Differential expression of the beta2-adrenergic receptor by Th1 and Th2 clones: implications for cytokine production and B cell help. *J Immunol* 1997;158:4200–10.

47 Daher C, Vimeux L, Stoeva R, *et al*. Blockade of β-Adrenergic Receptors Improves CD8+ T-cell Priming and Cancer Vaccine Efficacy. *Cancer Immunol Res* 2019;7:1849–63.

48 Knöferle J, Ramljak S, Koch JC, *et al*. TGF-beta 1 enhances neurite outgrowth via regulation of proteasome function and EFABP. *Neurobiol Dis* 2010;38:395–404.

49 Li S, Gu X, Yi S. The Regulatory Effects of Transforming Growth Factor-β on Nerve Regeneration. *Cell Transplant* 2017;26:381–94.

50 Batlle R, Andrés E, Gonzalez L, *et al*. Regulation of tumor angiogenesis and mesenchymal-endothelial transition by p38α through TGF-β and JNK signaling. *Nat Commun* 2019;10:3071.

51 Fridlender ZG, Sun J, Kim S, *et al*. Polarization of tumor-associated neutrophil phenotype by TGF-beta: 'N1' versus 'N2' TAN. *Cancer Cell* 2009;16:183–94.

52 Russell L, Swanner J, Jaime-Ramirez AC, *et al*. PTEN expression by an oncolytic herpesvirus directs T-cell mediated tumor clearance. *Nat Commun* 2018;9:5006.